Journal of Dental Sciences 19 (2024) 276–284

Available online at www.sciencedirect.com

ScienceDirect

journal homepage: www.e-jds.com

Original Article

# Assessment of rhBMP-2-loaded bovine hydroxyapatite granules in the guided bone regeneration of critical bone defect in rat mandible bone

J. López-Andaluz [a,1], J. Flores-Fraile [a,1], Javier-Borrajo [b], L. Blanco-Antona [a], R. García-Carrodeguas [c,d], D. López-Montañés [d], M.B. García-Cenador [a,d*], F.J. García-Criado [a,d]

[a] Department of Surgery, University of Salamanca, Salamanca, Spain
[b] Department of Physics, Engineering and Medical Radiology, University of Salamanca, Salamanca, Spain
[c] Department de R&D and Biomaterial Production, Noricum S.L, Madrid, Spain
[d] Biosanitary Research Institute (IBSAL), Salamanca, Spain

Received 16 February 2023; Final revision received 12 April 2023
Available online 28 April 2023

## Introduction

There is a pressing need to proceed with exogenous bone regeneration when the patient's spontaneous regenerative ability is insufficient. Numerous bone lesions involving a cavity repair themselves spontaneously, provided their size does not reach the so-called "critical bone cavity".

Regenerative medicine involves tissue engineering, using a matrix designed to act as a scaffold for supporting the regeneration process, creating a suitable microenvironment.[1] The scaffold is a key component, providing three-dimensional stability for cell interactions and an appropriate structure for the formation of the extracellular matrix, also serving as a carrier for releasing growth factors or transporting biochemical components to the receptor bed.[1]

The experimental bone scaffold Proteo-Graft (Noricum S.L.), hereafter PG, is used here. It consists of macroporous granules of bovine hydroxyapatite coated with a film of chitosan containing recombinant human bone morphogenetic protein type 2 (rhBMP-2) expressed in E. Coli. The granules of PG are expected to function as an osteoconductive bone scaffold supporting the adhesion and proliferation of mesenchymal stem cells (MSC), whereas rhBMP-2 stimulates and expedites their differentiation into osteoprogenitor cells. The bone morphogenetic protein (BMP-2) belongs to the family of transforming growth factor-beta (TGF-β), which is required for the bone's healing/regenerative ability. Sundry research teams are studying this role in the mediation of the cell response to biomaterials. The activation of the BMP-2/Smad4/RUNX2

* Corresponding author. Department of Surgery, University of Salamanca, Medical School, Avenida Alfonso X "El Sabio" s/n, Salamanca, 37007, Spain.
*E-mail address:* mbgc@usal.es (M.B. García-Cenador).
[1] These two authors contributed equally to this work.

https://doi.org/10.1016/j.jds.2023.04.016

signalling pathway promotes osteogenic differentiation and bone formation.[2]

Despite the wide array of bone substitutes and grafts available today, no definitive solution has thus far been found for the challenge of achieving fully satisfactory bone regeneration following their use. This research constitutes a step forward in the quest for new methods for total bone regeneration in cases of critical bone lesions.

## Materials and methods

### Experimental material

This study involved PG granules with a particle size of 1.0—0.25 mm (Lot M20001, Ref. PG1250.100/Noricum S.L. Madrid, Spain), composed of 99.2 wt% hydroxyapatite (bovine); 0.15 wt% acetic acid salts; 0.50 wt% chitosan; 0.15 wt% trehalose; and 0.05 wt% rhBMP-2.

### Study animals

This study was conducted according to both Spanish (Royal Decree 53/2013—Law 32/2007) and European Union (Directive 2010/63/EU) guidelines for the care and use of laboratory animals. Protocols were approved by the Ethics Committee on Animal Experimentation at the University of Salamanca (Licence Number: 361). Surgery was performed under monitored anaesthesia and all precautions were taken to minimise suffering. A total of 28 eight-month-old Wistar rats weighing 350 g were used here and randomly distributed into three groups:

- Simulated Group (GSh): Rats that underwent all the surgical procedures except for the cavitary bone lesion.
- Control Group (GC): all the surgical procedures including critical cavitary bone lesion, covering the bone defect with the membrane Evolution (OsteoBiol ® by Tecnoss, Turin, Italy).
- Study Group (GE): all the surgical procedures including critical cavitary bone lesion, filling the bone defect with PG (0.8 μg) and covering it with the OsteoBiol®.

They were euthanised at three or six months and samples were taken for studying the variables described (N = 12/6 in each case). Simulated Group (N = 4), at three months.

### Surgical technique

The rates were anaesthetised with an intraperitoneal injection containing xylazine (Rompun, Bayer, Leverkusen, Germany), ketamine chlorhydrate (Imalgene 1000, Rhone Méreuse, Lyon, France), and saline solution (ratio 2:3:3, at a dosage of 0.2 mL/100 g body weight). All the surgical procedures were performed under strict sterile conditions. A 15 mm longitudinal incision was made 2 mm above the lower edge of the mandibular body to expose the bone surface, gaining submandibular access to the specimen's ascendant mandibular branch and angle. A critical-sized defect (5 mm diameter) was made (Fig. 1).[3] Ostectomies

**Figure 1** Critical-sized rat mandibular bone defect model. After making an incision on the mandibular ramus, a full-thickness flap and reflection were created to expose the mandibular angle site. An experimental defect of 5 mm diameter was produced using a trephine drill on the right side of the mandible ramus.

were performed with an electric micromotor using a 5 mm trephine drill, with continuous irrigation with a physiological solution. The bone defect was then covered as described for each group. Animals were kept on a thermostatic blanket low noise model RTC-1 (Cibertec, Madrid, Spain), maintaining a temperature at 37 °C after surgery until they regained consciousness. An 0.05 mg/kg dose of buprenorphine (RB Pharmaceuticals Limited, Slough Berkshire, UK) was subcutaneously injected into the backs of the rats as an analgesia 1 h after surgery and then every 8 h for the following 72 h.

Post-surgical clinical monitoring was performed to assess the following: each specimen's overall health, the appearance of the wound and surgical area, any bleeding or discharge from the wound, and rejection of the biomaterials.

The following samples were obtained after 12 or 24 weeks:

- Whole blood by aortic puncture, with immediate centrifuging for 20′, 4500 rpm and 4 °C, extraction of the serum and storage at −80 °C.
- Perilesional tissue (bone and muscle), which was placed in liquid nitrogen and stored at −80 °C.
- Hemimandíbles (right and left), with some being submersed in formaldehyde, and others stored at −80 °C for the extraction of proteins.

### Macroscopic study

Descriptive evaluation of anatomy and tissue formation; signs of infection; fractures; presence or disappearance of the biomaterials; bone sequestration; surface morphology, and solidity of the defect.

### Study with microcomputed tomography (microCT)

Prior to their euthanasia, two specimens from the GC and GE groups were subject to a radiological assessment by means of a CT scan. The x-rays were transferred to the computer and digitised by shades of grey (16 bits). The programs used were the FIJI image processing package (distributed by IMAGE-J with added functions for image analysis), 3D Slicer platform, and IMAGE-J. The images were taken with a microCT SuperArgus device by SEDECAL Medical Systems at the Molecular Imaging Laboratory belonging to Salamanca University's Research Support Platform (NUCLEUS).

### Study with optical microscopy

The sections from each sample were stained with haematoxylin-eosin (H&E) and Masson's trichrome (MT) for their comparative histological study with optical microscopy.

### Immunohistochemical study

The osteogenesis of the lesions was obtained by processing the histological sections using indirect immunohistochemical techniques, which include incubating specific primary antibodies against the protein of interest and the addition of a biotinylated secondary antibody displayed by the standard ABC method using DAB as chromogen. The sections were analysed by optical microscopy (Leica DMLB) with an Olympus DP70 digital camera. The following osteogenic markers were analysed in the immunohistochemical study: RUNX2, alkaline phosphatase (ALP), and Osteocalcin (OCN), using the primary antibodies Anti-RUNX2 reference number: ab192256; Anti-ALP reference number: ab108337 (1:100; Abcam, Cambridge, UK), and Anti-OCN reference number: M65178420 (1:100; MyBioSource, San Diego, CA, USA).

### Study of BMP-2 with ELISA

One gram of bone tissue was ground and stored at −80 °C in 2 mL sampling tubes. The ground bone samples were then added to the solution aliquots (lysis buffer), being shaken until they dissolved. They were then boiled for 10 min and frozen at −80 °C. The samples were defrosted and then centrifuged at 14000 rpm for 10′ at 4 °C. The supernatant was removed and placed in 2-ml tubes. They were then sonicated for 10 s, aliquoted, and frozen at −80 °C.

For quantitative determination of BMP-2, a commercial enzyme-linked immunosorbent assay kit (ELISA) was used according to the manufacturer's instructions, reference number: DBP200 (R&D systems, Abingdon, UK).

### Statistical study

The quantitative data have been represented as X ± SD (mean ± standard deviation). A value of $P < 0.05$ was accepted as a significant result. The statistical software used for the study was NCSS 2007 and Gess 2006 - Version: 07.1.21 - Released 1 June 2011 (Dr Jerry L. Hintze, Kaysville, Utah, USA).

## Results

### Macroscopic results

The specimens recorded a 100% post-surgical survival rate, with a generally positive post-operative state of health, with no fractures. There was some swelling of the soft tissue due to the ostectomy, but it cleared spontaneously. As regards the biomaterials used, there was no rejection. The membrane recorded a suitable bio-reabsorption, low immunogenicity, stability, and lasting protection of the contingent graft covered.

### MicroCT results

The bone defect is clearly visible in the Control group (GC) at both three months (GC3) (Fig. 2 A) and at six (GC6) (Fig. 2 B). The specimens in the Study group (GE) at three months (GE3) (Fig. 3 C) did not present any signs of biomaterial integration. The bone defect was clearly identifiable, and the biomaterial appeared as an amorphous mass that filled the defect without integration. At six months (GE6) (Fig. 3D), the experimental material appeared to be better osseointegrated than in GE3, with difficulty in differentiating the bone tissue between the defect and the biomaterial.

### Histological results

The histological images for GC (Fig. 4) reveal a fibrous scarring reaction in the untreated lesion area at both three and six months, which indicates scant bone regeneration activity. GE3 (Fig. 5) revealed a large amount of biomaterial granules distributed throughout the sample area, lightly stained by the haematoxylin, with a reddish hue in the MT preparations. There was a greater formation of immature bone tissue filling both the critical defect and the spaces between the biomaterial granules compared to GC. No inflamed tissue was found and there was hardly any fibrous tissue. The biomaterial appears as an amorphous mass and no osteoclastic activity was detected. There was a large amount of reactive connective tissue consisting of fibroblasts and collagen fibres, with some young, short, and isolated trabeculae near the external and interior surface of the cortical, as well as between the biomaterial granules. No osteoblasts or osteoclasts were found. The collagen tissue and immature bone were stained in red with MT, while the muscle tissue and the mature lamellar bone were stained green.

The histological images for GE6 (Fig. 6) manifested a higher degree of bone neoformation as immature bone

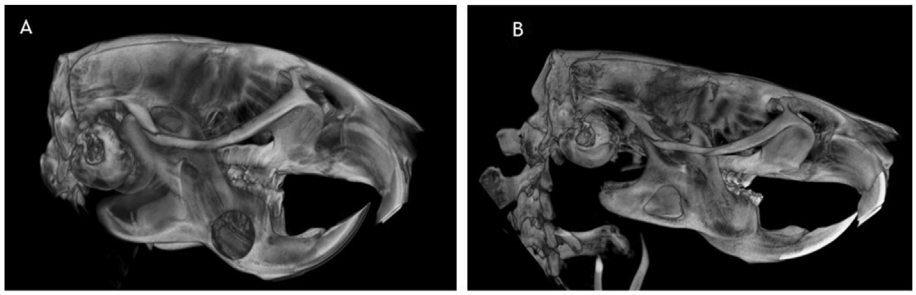


**Figure 2** Tomographic evaluation of the mineralisation for the mandibular bone defect control group with OsteoBiol® (GC). The images present the gross mineralisation for the control groups by computerised tomography (microCT) at the observation intervals of three and six months after surgery (GC3 and GC6). (A. Aspect of the critical defect in GC3. B. Aspect of the critical defect in GC6). Image B shows there is newly formed bone six months after surgery only along the defect borders, as compared to image A three months after surgery.

tissue, compared to the histological sections for GC3 and GE3. A highlight was the greater formation of bone tissue in the defect and within the medullar channel compared to the sections for GC3 and GE3. No osteoclastic or inflamed tissue was detected. The percentage of biomaterial differed between GE3 and GE6, with almost all the biomaterial being reabsorbed at six months (Fig. 6D).

### BMP-2 results

The BMP-2 results obtained with ELISA are presented in Table 1.

The bone lesion stimulated the production of BMP-2, which decreased over the passage of time (as shown by the increase in BMP-2 in GC3 compared to GSh and by the absence of differences between GSh and GC6 and the differences between GC3 and GC6) (Fig. 7). The administration of the treatment in GE3 and GE6 increased the amount of BMP-2, which decreased significantly over the passage of time (as shown by the increase in BMP-2 in GE3 and GE6 compared to GSh, GC3, and GC6 and by the higher amount detected in GE3 compared to GE6) (Fig. 7).

### Immunohistochemical results

The osteogenic markers studied were as follows: RUNX2 and OCN and ALP. Given the non-formation of bone tissue, the immunohistochemical images for GC (Fig. 8) have no ALP, OCN, or RUNX2 expression at either three or six months. Nevertheless, the staining results for GE3 and GE6 reveal clearer positive areas that reflect the expression of osteogenic markers (Fig. 9). The ALP expression is higher in the cytoplasm of the osteoblasts in GE3 (Fig. 9A), and there is no detectable expression in GE6 (Fig. 9D). The levels of OCN at three months, as shown in Fig. 11B, are higher in GE6 (Fig. 9E). The positive staining of RUNX2 (Fig. 9C) and OCN (Fig. 9B) was clearly accumulated in the newly formed collagen and in the bone tissue. The lower level of these osteoblastic and osteogenic markers at six months (Fig. 9 D, E and F) may be because after three months the defects were covered mainly by new bone.

## Discussion

There is currently an increase in the pathology associated with the loss of bone mass and fractures caused by fragility.[4] Moreover, a significant percentage of these cases, between 5% and 50%, do not evolve favourably on their own and require surgery.[5] There are advantages and drawbacks to the different grafts; their therapeutic future involves the use of biocompatible alloplastic materials that have the fewest drawbacks and the most benefits for patients, favouring tissue regeneration and expediting processes.[6]


**Figure 3** Tomographic evaluation of the mineralisation for the mandibular bone defect study group (GE), with experimental bone scaffold Proteo-Graft 0,8 μg (PG). The images present the gross mineralisation for the study groups by computerised tomography (microCT), at the observation intervals of three and six months after surgery (GE3 and GE6). (C. Aspect of the critical defect in GE3. D. Aspect of the critical defect in GE6). Radiopacity provides visual and descriptive follow-up of the bone defect. There is more biomaterial in image C than in image D.

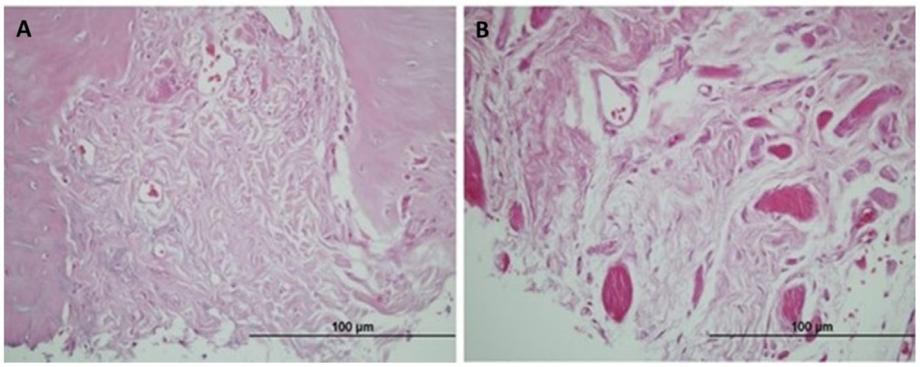


**Figure 4** H&E stained images for the critical size mandibular bone defect control group with OsteoBiol® (GC) at three (GC3) and six months (GC6). Cross-sectional cut at a central region and edge of the defect. A. Haematoxylin-eosin in GC3. B. Haematoxylin-eosin in GC6. Scale bars in figures indicate 100 µm. Only mild new bone formation was embedded in connective tissue spanning the edge of the defect, as seen in image B.

This study has sought to assess the performance of an experimental three-dimensional matrix in the regeneration of a critical mandibular defect in rats, corresponding to an area of 5 × 2 mm (diameter × depth) in rat mandible near the alveolar zone.[3] The defects inflicted did not lead to spontaneous regeneration, and are therefore valid for studying bone neoformation materials and bone substitutes.[7] Furthermore, it is readily reproducible, highly effective, and economical.

Following the graft, the material gradually degrades over a period of three to six months subsequent to surgery.[8,9] This degradation begins on the periphery of the

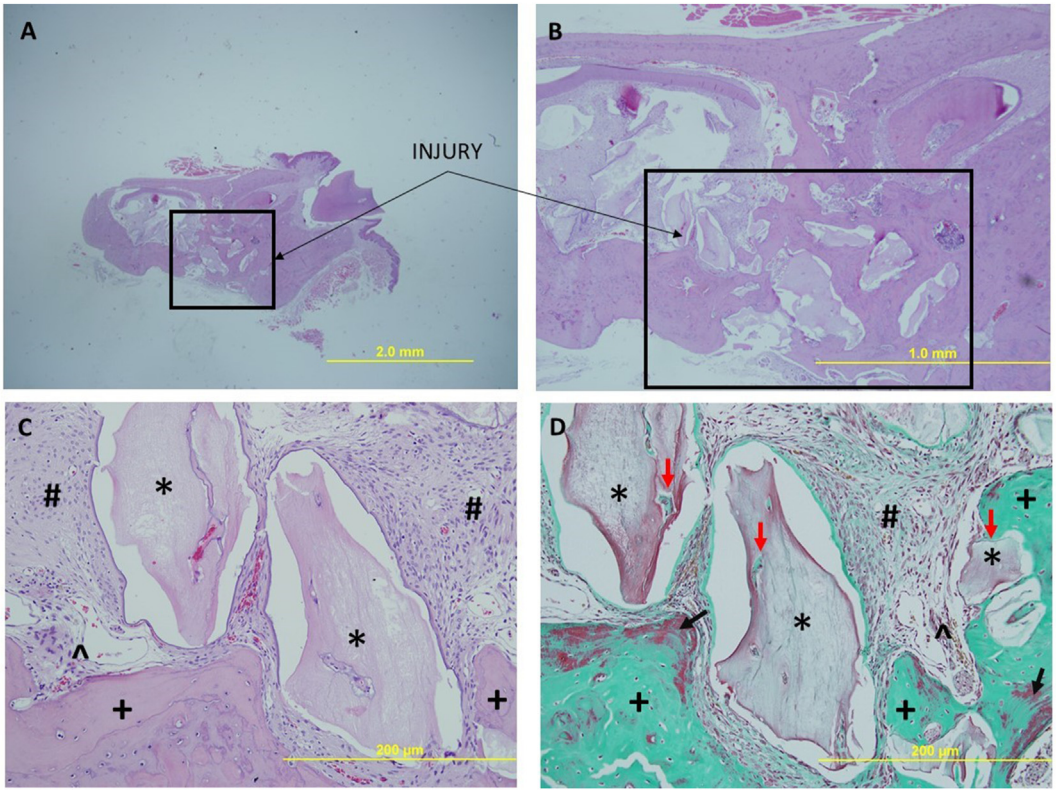


**Figure 5** H&E and MT stained images for the critical size mandibular bone defect study group with PG (0,8 µg) at three months (GE3). Scale bars indicate 2.0 mm in figure A, 1.0 mm in figure B, and 200 µm in figure C. Biomaterial*; Neoformed bone tissue filling the defect and the spaces between the biomaterial granules (osteocytes and vessels) +; Reactive connective tissue (collagen and fibroblasts) #; Bone (osteoblasts and vessels) ^; MT stain D (200 µm). Reactive connective tissue (collagen and fibroblasts)#; Bone matrix (osteoblasts and vessels)^; Bone in dark green. Neoformed immature bone tissue in red (black arrow); Neoformed bone tissue in contact with the biomaterial (red arrows). (For interpretation of the references to colour in this figure legend, the reader is referred to the Web version of this article.)

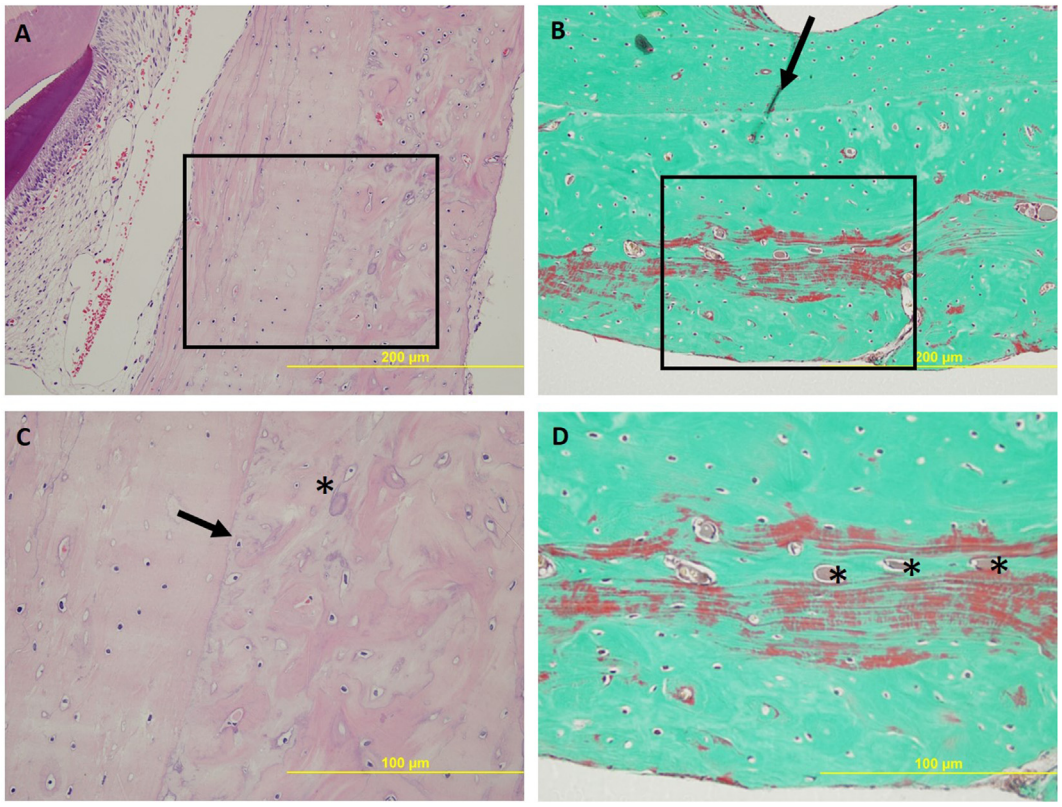


**Figure 6** H&E and MT stained images for the critical size mandibular bone defect study group with PG (0.8 µg) at six months (GE6). Scale bars indicate 200 µm in figure A and 100 µm in figure C. Biomaterial*; Neoformed bone tissue filling the defect and the few spaces between the biomaterial granules; edge of the defect (black arrow). MT stain B (200 µm) and D (100 µm). Bone in dark green. Immature neoformed bone tissue in red; Neoformed bone tissue in contact with the scarce amount of biomaterial. (For interpretation of the references to colour in this figure legend, the reader is referred to the Web version of this article.)

implanted material and extends inwards towards the core. The descriptive analysis with microCT observed a gradual breakdown of the biomaterial's initial morphology, accompanied by the neoformation of the bone tissue in GE3. However, this descriptive analysis does not detect the evolution of the connecting matrix, nor the temporal development of the biomaterial's degradation, or bone dispersion/neoformation. These issues have been highlighted by conducting histological analysis, and the data forthcoming have revealed histological differences between GC and GE.

The membrane recorded suitable bio-reabsorption, low immunogenicity, stability, and lasting protection of the contingent graft covered. In histological terms, GC3 manifested a fibrotic formation due to the release of inflammatory mediators following the defect caused. There were no signs of regeneration, corroborated by the radiological tests, and the osteocytes surrounding the lesion necrotise and die due to ongoing hypoxia and the absence of capillaries. This difference in the results for the study groups reveals an increase in the density of the lesion area, with no signs of inflammation or an allergic reaction.

GE3 records osteogenic activity, with high cellularity, and there are biomaterial granules surrounded by trabeculae of osteoid matrix that include some osteoblasts (which begin calcifying it), with detection also of osteoblast precursor cells and mature osteocytes in the ossification line. GE6 reveals an organised bone structure, with complete regeneration and a well-vascularised haversian structure. There is adult bone, which maintains the original dimensions, and two different zones, mature bone tissue characterised by its bone structure (mineralised interstitial substance) that is organised forming bone lamellae. There are osteocytes in the spaces in the lacunae, arranged like the lamellae in a concentric and parallel manner. There is neoformed bone tissue that contains a relatively higher proportion of osteocytes, with larger lacunae than those appearing in the mature bone, and the collagen fibres following several directions.

**Table 1** BMP-2 results. Quantitative expression of BMP2 in each group at three and six months.

| | GSh | GC3 | GC6 | GE3 | GE6 |
|---|---|---|---|---|---|
| BMP-2 (pg/mL) | 200.45 ± 6.78 | 494.20 ± 61.54 | 306.92 ± 33.89 | 2438.01 ± 170.98 | 852.36 ± 90.20 |

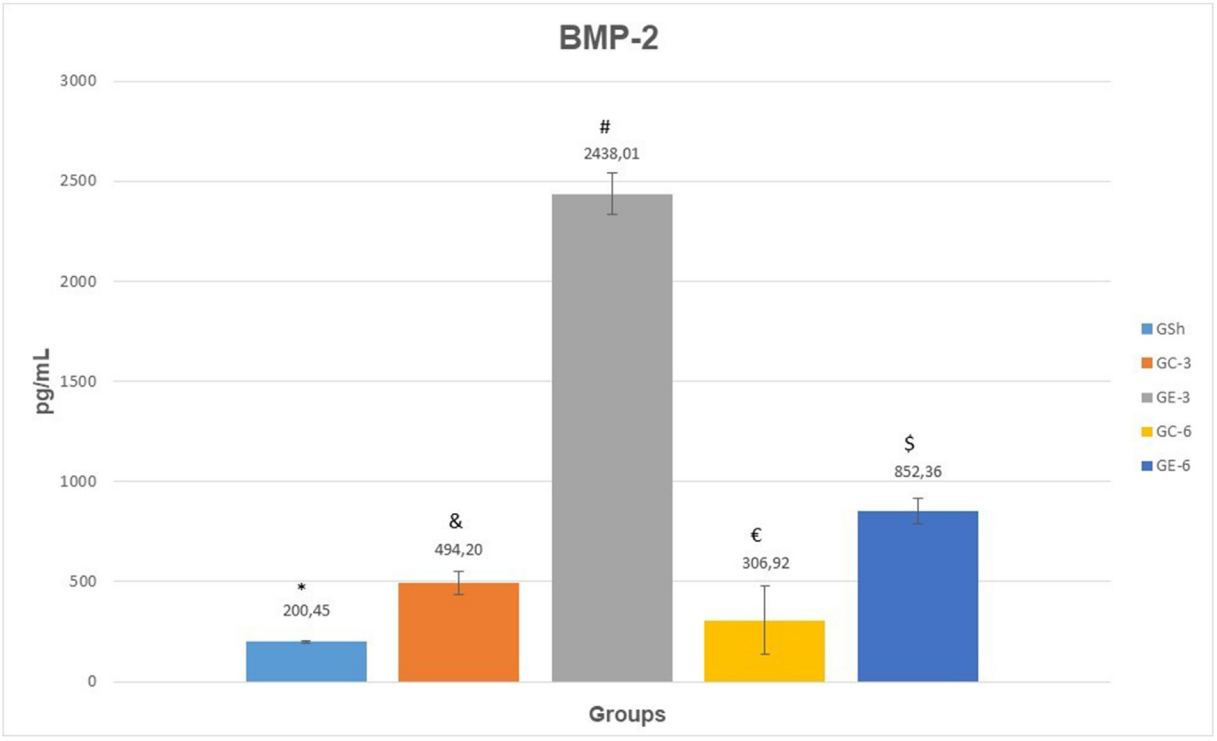


**Figure 7** Protein expression of BMP2 in each group at three and six months. ANOVA (Scheffe's test and Tukey-Kramer test), was used to determine statistical significance. The data shown represent the means ± SD (n = 6). $P < 0.05$, comparing all groups. (* Different to GC3, GE3, GE6 — and different to GSh, GC6, GE3, GE6 - # Different to GSh, GC3, GC6, GE6 - € Different to GC3, GE3, GE6 - $ Different to GSh, GC3, GC6, GE3).

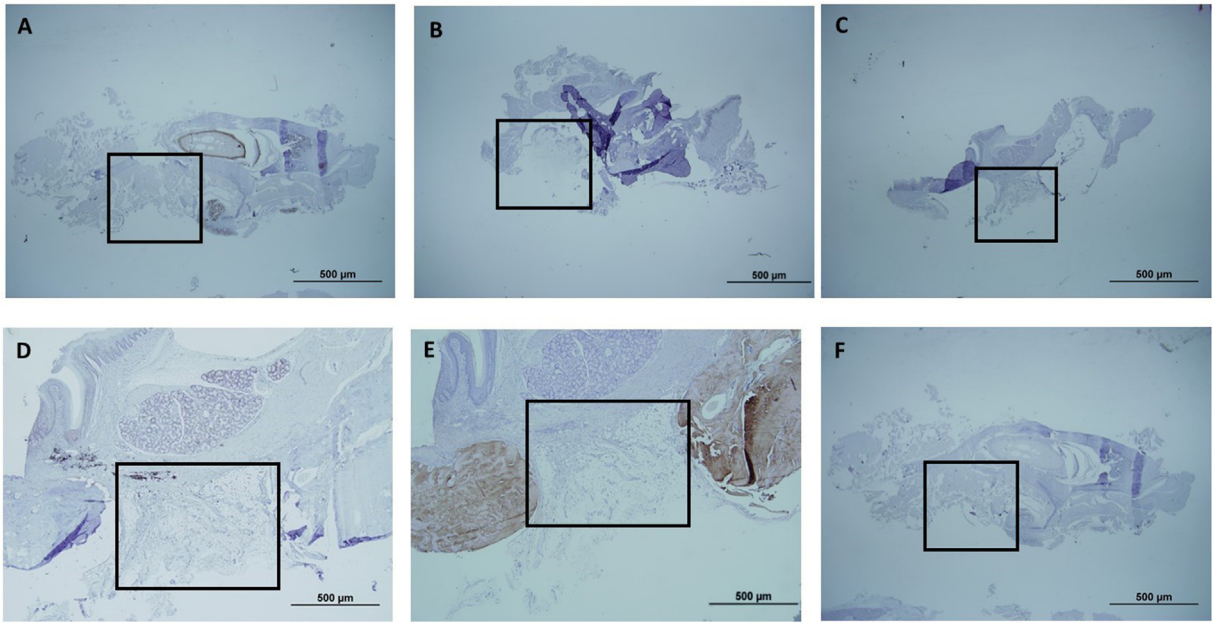


**Figure 8** Immunohistochemical staining of osteogenic markers in rat mandibular bone defect control group with OsteoBiol® (GC) at three (GC3) and six months (GC6). Scale bars in images indicate 500 µm. The immunohistochemistry results for protein expression of osteogenesis in bone at three and six months, (A and D, ALP. B and E, OCN. C and F, RUNX2). No detectable expression of ALP at three months A or at six months D, nor of OCN and RUNX2 at three months, B and C, or at six months E and F. The absence of immunoreactivity for ALP, OCN and RUNX2 proteins was evident in the control groups given the non-formation of bone tissue.

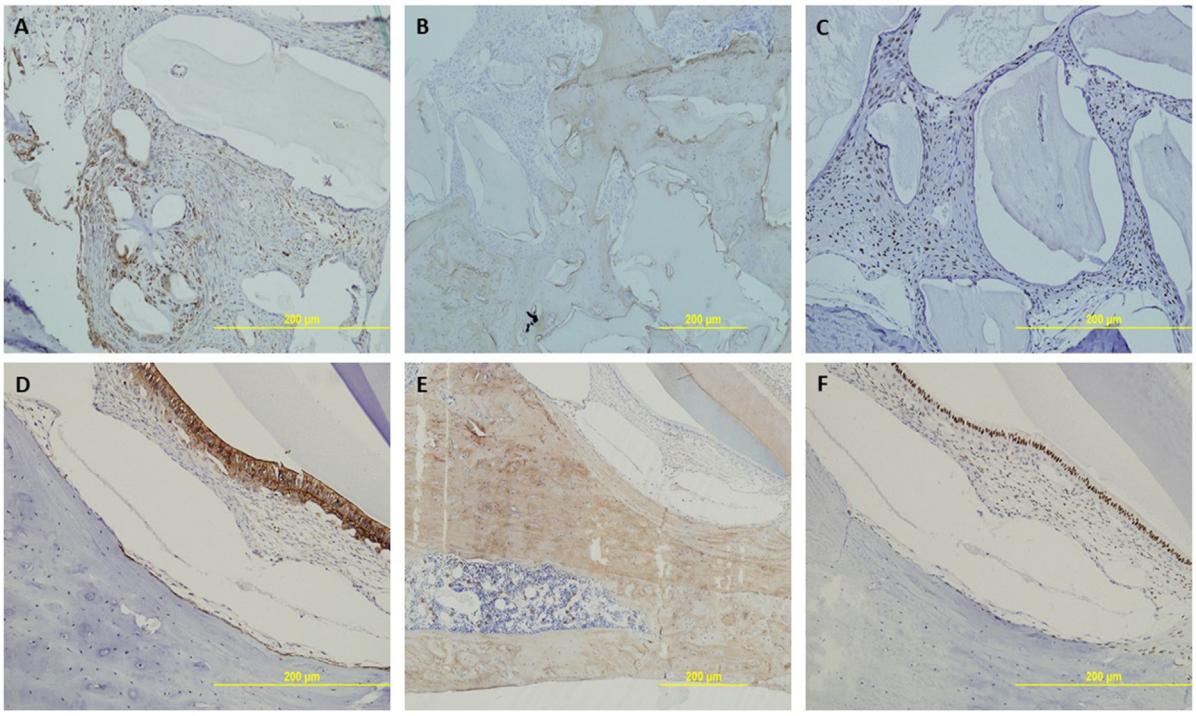


**Figure 9** Immunohistochemical staining of osteogenic markers in rat mandibular bone defect study group with PG (0.8 μg) at three (GE3) and six months (GE6). Scale bars in images indicate 200 μm. The immunohistochemistry results for protein expression of osteogenesis in bone at three months: A, Expression of ALP located in the cytoplasm of the osteoblasts, B, OCN attached to the hydroxyapatite of the biomaterial and C, RUNX2 in the cytoplasm of the pre-osteoblasts. At six months: D, No detectable expression of ALP, or of OCN, E and RUNX2, F. In contrast, the absence of immunoreactivity for ALP, OCN and RUNX2 proteins at six months may be because the defects were covered by new bone.

The biomaterial used, PG, contains 0.05 wt% of rhBMP-2. The level of BMP-2 in bone tissue at the implant site was studied in GC and GE, manifesting a greater expression in GE3, whereby this molecule is effective after being implanted, prompting bone regeneration in the critically sized mandible defect. The level of osteogenic activity in GE3 and GE6 could therefore be directly linked to the action of BMP-2.[10] The evidence shows that the administration of BMP-2 favours angiogenesis and osteogenesis, contributing to bone regeneration.[11] BMP-2 is an extracellular signalling molecule, an *in vivo* autocrine/paracrine factor[12] that promotes osteoregeneration and induces the differentiation of osteoblasts and the formation of bone, cartilage, and connective tissue. These outcomes, in turn, lead to an increase in the osteoinductive capacity of BMP-2 at local level.[13] Neovascularisation through specific paracrine pathways leads to the formation of angiogenic growth factors, producing more osteoblasts and BMP-2 through two-way coupling.[14] This prompts a crucial initial angiogenesis in the osteogenesis.[15] BMP-2 is therefore the most effective inductor in the differentiation of osteoblast bone formation, and it regulates the activation of the BMP-2/Smad/RUNX2 signalling pathway, increasing the RUNX2 expression,[12] which is an important transcription factor in the differentiation of osteoblasts. The positive effect of the experimental biomaterial PG on bone regeneration, manifested in the histological results, is probably because BMP-2 favours the circulation of stem cells,[16] the spread of fibroblasts, and type I collagen synthesis.[17]

The osteogenic markers ALP, RUNX2, and OCN were chosen for the study because they are expressed in the different stages of osteogenesis.[18–20] ALP is an early osteogenic marker,[21] and its activity was studied to determine the early degree of osteoblast differentiation.[21,22] The immunohistochemical results of ALP reported here were expressed in GE3 but not, however, in GC3, GC6, or GE6. RUNX2 is an important transcription factor in the differentiation of osteoblasts. OCN is produced solely by mature osteoblasts and plays an important role in bone mineralisation. The low level of this osteoblastic marker may be because after three months the defects were covered mainly by new bone.[6] The immunohistochemical results reported reveal an increased expression of the osteoblastic markers RUNX2 and OCN in both GEs, which will therefore favour osteogenesis mediated by BMP-2 contributing to the regeneration of the mandibular lesion. A clinical trial is currently being conducted to assess the safety and efficacy of PG as a bone substitute in alveolar socket regeneration (Regeneration of Alveolar Sockets with rhBMP-2-Loaded Bovine Bone Mineral (Proteo-Graft). ClinicalTrials.gov identifier: NCT05717478).

This study has shown that the experimental material used promotes the structural restitution of the critical bone defect with newly regenerated bone over the timeframe studied in Wistar rats due to the large osteogenic and angiogenic capacity of BMP-2 contained in PG. Nonetheless, further research is called for on action mechanisms, therapeutic dosages, and other possible variables that might affect the results.

## Declaration of competing interest

The authors have no conflicts of interest relevant to this article.

## References


1. Molina MIE, Malollari KG, Komvopoulos K. Design challenges in polymeric scaffolds for tissue engineering. *Front Bioeng Biotechnol* 2021;9:617141.
2. Zhang GL, Liu WJ, Wang RL, et al. The role of tantalum nanoparticles in bone regeneration involves the BMP2/Smad4/Runx2 signaling pathway. *Int J Nanomed* 2020;15:2419—35.
3. Kim JH, Kim HW. Rat defect models for bone grafts and tissue engineered bone constructs. *Tissue Eng Regen Med* 2013;10:310—6.
4. Aguado HJ, Castillón-Bernal P, Ventura-Wichner PS, et al. Impact of subtrochanteric fractures in the geriatric population: better pre-fracture condition but poorer outcome than pertrochanteric fractures: evidence from the Spanish Hip Fracture Registry. *J Orthop Traumatol* 2022;23:17.
5. Condorhuamán-Alvarado PY, Pareja-Sierra T, Muñoz-Pascual A, et al. Improving hip fracture care in Spain: evolution of quality indicators in the Spanish National Hip Fracture Registry. *Arch Osteoporosis* 2022;17:54.
6. Bahraminasab M, Doostmohammadi N, Talebi A, et al. 3D printed polylactic acid/gelatin-nano-hydroxyapatite/platelet-rich plasma scaffold for critical-sized skull defect regeneration. *Biomed Eng Online* 2022;21:86.
7. Sargolzaei-Aval F, Saberi EA, Arab MR, Sargolzaei N, Sanchooli T, Tavakolinezhad S. Octacalcium phosphate/gelatin composite facilitates bone regeneration of critical-sized mandibular defects in rats: a quantitative study. *J Dent Res Dent Clin Dent Prospects* 2019;13:258—66.
8. Sweedy A, Bohner M, Baroud G. Multimodal analysis of in vivo resorbable CaP bone substitutes by combining histology, SEM, and microcomputed tomography data. *J Biomed Mater Res B Appl Biomater* 2018;106:1567—77.
9. Seyedsalehi A, Daneshmandi L, Barajaa M, Riordan J, Laurencin CT. Fabrication and characterization of mechanically competent 3D printed polycaprolactone-reduced graphene oxide scaffolds. *Sci Rep* 2020;10:22210.
10. Kim CH, Ju MH, Kim BJ. Comparison of recombinant human bone morphogenetic protein-2-infused absorbable collagen sponge, recombinant human bone morphogenetic protein-2-coated tricalcium phosphate, and platelet-rich fibrin-mixed tricalcium phosphate for sinus augmentation in rabb. *J Dent Sci* 2017;12:205—12.
11. Yao H, Guo J, Zhu W, et al. Controlled release of bone morphogenetic protein-2 augments the coupling of angiogenesis and osteogenesis for accelerating mandibular defect repair. *Pharmaceutics* 2022;14:2397.
12. Ren S, Jiao G, Zhang L, You Y, Chen Y. Bionic tiger-bone powder improves bone microstructure and bone biomechanical strength of ovariectomized rats. *Orthop Surg* 2021;13:1111—8.
13. Pearson HB, Mason DE, Kegelman CD, et al. Effects of bone morphogenetic protein-2 on neovascularization during large bone defect regeneration. *Tissue Eng* 2019;25:1623—34.
14. Bedeloğlu E, Ersanlı S, Arısan V. Vascular endothelial growth factor and biphasic calcium phosphate in the endosseous healing of femoral defects: an experimental rat study. *J Dent Sci* 2017;12:7—13.
15. Silva AS, Santos LF, Mendes MC, Mano JF. Multi-layer prevascularized magnetic cell sheets for bone regeneration. *Biomaterials* 2020;231:119664.
16. Katagiri W, Takeuchi R, Saito N, Suda D, Kobayashi T. Migration and phenotype switching of macrophages at early-phase of bone-formation by secretomes from bone marrow derived mesenchymal stem cells using rat calvaria bone defect model. *J Dent Sci* 2022;17:421—9.
17. Guo T, Yuan X, Li X, Liu Y, Zhou J. Bone regeneration of mouse critical-sized calvarial defects with human mesenchymal stem cell sheets co-expressing BMP2 and VEGF. *J Dent Sci* 2023;18:135—44.
18. Fu C, Yang X, Tan S, Song L. Author Correction: enhancing cell proliferation and osteogenic differentiation of MC3T3-E1 pre-osteoblasts by BMP-2 delivery in graphene oxide-incorporated PLGA/HA biodegradable microcarriers. *Sci Rep* 2020;10:6249.
19. Schini M, Vilaca T, Gossiel F, Salam S, Eastell R. Bone turnover markers: basic biology to clinical applications. *Endocr Rev* 2022;13. bnac031.
20. Furuhata M, Takayama T, Yamamoto T, et al. Real-time assessment of guided bone regeneration in critical size mandibular bone defects in rats using collagen membranes with adjunct fibroblast growth factor-2. *J Dent Sci* 2021;16:1170—81.
21. Zhou P, Shi JM, Song JE, et al. Establishing a deeper understanding of the osteogenic differentiation of monolayer cultured human pluripotent stem cells using novel and detailed analyses. *Stem Cell Res Ther* 2021;12:41.
22. Gonzalez-Pujana A, Carranza T, Santos-Vizcaino E, et al. Hybrid 3D Printed and electrospun multi-scale hierarchical polycaprolactone scaffolds to induce bone differentiation. *Pharmaceutics* 2022;14:2843.